The feasibility of a scanner-independent technique to estimate organ dose from MDCT scans: Using $CTDI_{vol}$ to account for differences between scanners

Adam C. Turner[a)]
Departments of Biomedical Physics and Radiology, David Geffen School of Medicine, University of California, Los Angeles, Los Angeles, California 90024

Maria Zankl
Helmholtz Zentrum München, Institute of Radiation Protection, German Research Center for Environmental Health (GmbH), Ingolstaedter Landstraße 1, 85764 Neuherberg, Germany

John J. DeMarco
Department of Radiation Oncology, University of California, Los Angeles, Los Angeles, California 90095

Chris H. Cagnon, Di Zhang, and Erin Angel
Departments of Biomedical Physics and Radiology, David Geffen School of Medicine, University of California, Los Angeles, Los Angeles, California 90024

Dianna D. Cody
Department of Imaging Physics, University of Texas M. D. Anderson Cancer Center, Houston, Texas 77030

Donna M. Stevens
Oregon Health Sciences University, Portland, Oregon 97239

Cynthia H. McCollough
Department of Radiology, Mayo Clinic College of Medicine, Rochester, Minnesota 55901

Michael F. McNitt-Gray
Departments of Biomedical Physics and Radiology, David Geffen School of Medicine, University of California, Los Angeles, Los Angeles, California 90024

(Received 10 August 2009; revised 9 February 2010; accepted for publication 1 March 2010; published 29 March 2010)

Purpose: Monte Carlo radiation transport techniques have made it possible to accurately estimate the radiation dose to radiosensitive organs in patient models from scans performed with modern multidetector row computed tomography (MDCT) scanners. However, there is considerable variation in organ doses across scanners, even when similar acquisition conditions are used. The purpose of this study was to investigate the feasibility of a technique to estimate organ doses that would be scanner independent. This was accomplished by assessing the ability of $CTDI_{vol}$ measurements to account for differences in MDCT scanners that lead to organ dose differences.

Methods: Monte Carlo simulations of 64-slice MDCT scanners from each of the four major manufacturers were performed. An adult female patient model from the GSF family of voxelized phantoms was used in which all ICRP Publication 103 radiosensitive organs were identified. A 120 kVp, full-body helical scan with a pitch of 1 was simulated for each scanner using similar scan protocols across scanners. From each simulated scan, the radiation dose to each organ was obtained on a per mA s basis (mGy/mA s). In addition, $CTDI_{vol}$ values were obtained from each scanner for the selected scan parameters. Then, to demonstrate the feasibility of generating organ dose estimates from scanner-independent coefficients, the simulated organ dose values resulting from each scanner were normalized by the $CTDI_{vol}$ value for those acquisition conditions.

Results: $CTDI_{vol}$ values across scanners showed considerable variation as the coefficient of variation (CoV) across scanners was 34.1%. The simulated patient scans also demonstrated considerable differences in organ dose values, which varied by up to a factor of approximately 2 between some of the scanners. The CoV across scanners for the simulated organ doses ranged from 26.7% (for the adrenals) to 37.7% (for the thyroid), with a mean CoV of 31.5% across all organs. However, when organ doses are normalized by $CTDI_{vol}$ values, the differences across scanners become very small. For the $CTDI_{vol}$, normalized dose values the CoVs across scanners for different organs ranged from a minimum of 2.4% (for skin tissue) to a maximum of 8.5% (for the adrenals) with a mean of 5.2%.

Conclusions: This work has revealed that there is considerable variation among modern MDCT scanners in both $CTDI_{vol}$ and organ dose values. Because these variations are similar, $CTDI_{vol}$ can be used as a normalization factor with excellent results. This demonstrates the feasibility of establishing scanner-independent organ dose estimates by using $CTDI_{vol}$ to account for the differences

between scanners. © *2010 American Association of Physicists in Medicine*.
[DOI: 10.1118/1.3368596]

Key words: CT, multidetector row CT, radiation dose, organ dose, Monte Carlo simulations

I. INTRODUCTION

Recent studies report that from 1993 to 2006 the number of computed tomography (CT) imaging procedures increased at an annual rate of over 10% in the United States, leading to a considerable increase in the collective radiation dose from CT.[1] Specifically, CT exams now constitute 15% of the total number of radiological imaging procedures, but contribute more than 50% of the population's medical radiation exposure.[1] It has been suggested that the most appropriate quantity for assessing the risk due to diagnostic imaging procedures is the radiation dose to individual organs.[2–6] These findings suggest that a method to quickly and accurately determine the dose delivered to the individual organs of patients undergoing CT examinations would be extremely useful in a clinical setting.

The currently accepted method for monitoring radiation dose from CT is based on the use of the CT dose index (CTDI), which is meant to be a directly measurable estimate of the average dose from a multiple-scan examination.[7] These measurements are obtained using an ionization chamber placed a in polymethyl methacrylate (PMMA) cylindrical phantoms.[7,8] CTDI values are widely used for quality assurance and accreditation purposes; however, they are not intended to represent dose to any particular patient or, more importantly, to any particular organ.[7–9]

To estimate radiation dose to organs, Monte Carlo radiation transport codes have been developed to simulate CT examinations and can be used with a wide array of computational anthropomorphic phantoms. The Monte Carlo simulation approach was used in dosimetry studies performed by both the NRPB (Chilton, U.K.)[10] and the GSF (Oberschleissheim, Germany),[11] the results of which have been incorporated into software packages such as the IMPACT CT Patient Dosimetry Calculator (ImPACT, London, England)[12] and CT-EXPO (Medizinische Hochschule, Hannover, Germany).[13] While the original studies were based on single detector row, nonhelical scanners, methods to extend the results to current, commercially available helical CT scanners have been developed, for example, by matching new scanners to those originally simulated based on physical measurements (such as CTDI).[12] While these methods exist to estimate organ dose, differences between the NRPB mathematical phantoms and actual patient models as well as inaccuracies resulting from approximating doses to helical scanners from axial scanners using scanner matching techniques may result in inaccurate dose estimates.[14,15]

An alternative approach for estimating radiation dose, based on CTDI to dose conversion coefficients, was previously suggested by Shrimpton.[16] This approach was predicated on his observation that the normalization of effective doses from the NRPB Monte Carlo data sets by weighted CTDI ($CTDI_w$) accounted for scanner differences that contributed to dose disparities among axial CT scanner models.[16] According to Shrimpton, these results suggest the feasibility of scanner-independent $CTDI_w$ to organ dose conversion coefficients for estimating doses from any axial scanner in a standardized fashion. This would be similar to the use of region-specific *k*-factors (effective dose per DLP) for estimating effective dose [as described in AAPM Report 96 (Ref. 3) and others[17–19]] but would allow specific organ dose estimates to be obtained.

More recently, Monte Carlo dosimetry packages dedicated to simulating modern multidetector row CT (MDCT) scanners have been developed that utilize very detailed computational anthropomorphic models generated based actual patient images.[14,15,20–25] However, it has been problematic to conduct a comprehensive study of organ dose values for a number of different MDCT scanners in order to assess cross-scanner dose variations. This is primarily due to the difficulty in obtaining the necessary, but often proprietary, information to model specific scanners, such as x-ray source information (e.g., energy spectrum and filtration design). Recent work by Turner, *et al.* demonstrated a method to generate "equivalent" x-ray source models which resulted in accurate dosimetry simulations for 64-slice scanners from all four major scanner manufacturers when utilized by a previously presented Monte Carlo radiation transport package.[20,26] The conclusions of these studies imply that it is possible to obtain accurate organ dose values from 64-slice MDCT scanners from any manufacturer.

The purpose of this study was to investigate the feasibility of a technique to estimate organ doses that would be scanner-independent. This was accomplished by first carrying out Monte Carlo dosimetry simulations of multiple 64-slice MDCT scanners on a single patient model to acquire organ doses. Then, for each scanner, standard $CTDI_{vol}$ values were measured and used as normalization factors for the simulated organ doses. Finally, the variations across scanners of $CTDI_{vol}$ values, un-normalized organ doses, and $CTDI_{vol}$ normalized organ doses were computed. The results will allow conclusions to be drawn regarding the utility of using $CTDI_{vol}$ to account for scanner differences influencing organ dose and ultimately assess the feasibility of generating scanner-independent $CTDI_{vol}$ to organ dose conversion coefficients for MDCT scanners.

II. MATERIALS AND METHODS

II.A. The CT scanners

This study included 64-slice MDCT scanners from four major CT scanner manufacturers: The LightSpeed VCT (General Electric Medical Systems, Waukesha, WI), SOMATOM Sensation 64 (Siemens Medical Solutions, Inc.,

Forcheim, Germany), Brilliance CT 64 (Philips Medical Systems, Cleveland, OH), and Aquilion 64 (Toshiba Medical Systems, Inc., Otawara-shi, Japan). Each of these is a third generation MDCT scanner that supports multiple nominal beam collimation settings as well as multiple beam energies. All scanners are equipped with x-ray beam filtration that includes from one to three available bowtie filters. For this work, all experiments were carried out with a tube voltage of 120 kVp and the bowtie filter designed for the adult body. In order to select comparable collimation widths, the widest available collimation setting for each scanner was used for all experiments; it should be noted that the widest available collimation typically has the largest dose efficiency (highest ratio of nominal total collimated beam width to actual measured beam width). Therefore, the selected nominal collimation settings used were 40 mm (i.e., 64×0.625 mm^2) for the LightSpeed VCT and Brilliance CT 64, 32 mm (i.e., 64×0.5 mm^2) for the Aquilion 64, and 28.8 mm (i.e., 24×1.2 mm^2) for the Sensation 64 scanners, respectively. The organ dose simulations described below were performed for helical scans with a pitch value of 1 (even if the scanner cannot actually perform a scan of pitch 1). Each scanner was randomly assigned an index number, either 1, 2, 3, or 4, and will be referred to by its assigned index from this point on.

II.B. CTDI measurements

Conventional CTDI measurements were performed to obtain $CTDI_{100}$ and $CTDI_{vol}$ values, for scanners 1–4. All measurements were made with a standard 100 mm pencil ionization chamber (ion chamber) and a calibrated electrometer. The $CTDI_{100}$ values were obtained at both the center and periphery (12 o'clock) positions in a 32 cm diameter (body) CTDI phantom using the scanner settings described in Sec. II A. Each $CTDI_{100}$ measurement was acquired using a sufficiently high mA s value (ranging from 200–300 mA s/rotation) and was reported on a per mA s value. Specifically, scanner-specific $CTDI_{100}$, denoted $CTDI_{100,S}$, was obtained by measuring the exposure (E) from a single axial scan and calculated (in mGy/mA s) using Eq. (1)

$$CTDI_{100,S}=\frac{f\times C\times E\times L}{N\times T}\times\frac{1}{\beta}, \quad (1)$$

where f is the conversion factor from exposure to a dose in air (8.7 mGy/R), C is the calibration factor for the electrometer, L is the active length of the ionization chamber (100 mm), $N\times T$ is the nominal collimation width, and β is the actual mA s/rotation value used for the measurement. The corresponding $CTDI_{vol,S}$, also in mGy/mA s, pertaining to a helical scan with a pitch of 1 was then determined for scanners 1–4 as described by McNitt-Gray.[8]

II.C. Overview of the Monte Carlo method

II.C.1. Monte Carlo simulations

All simulations were performed using the MCNPX (MCNP eXtended v2.7.a) Monte Carlo radiation transport code.[27,28] The simulations used in this work were executed in photon mode with a low-energy cutoff of 1 keV. For this work, we ignore photoelectrons and assume all deposited energy is absorbed at the photon interaction site. This assumption satisfies the condition of charged particle equilibrium (CPE) for which the collision kerma is equal to absorbed dose and has shown to be valid for the diagnostic x-ray energy range.[20] The photon energy fluence (ψ) was scored for each simulated photon in regions of interest using the MCNPX *F4 tally and converted to absorbed dose by multiplying by the energy dependent mass energy-absorption coefficients, (μ_{en}/ρ), reported by Hubbell and Seltzer[29] using the MCNPX dose energy (DE) and dose function (DF) cards.

II.C.2. Modeling of the CT source

MCNPX requires the initial position, trajectory, and energy of each simulated photon to be specified. Modifications were made to the standard code to randomly sample from all possible starting positions corresponding to a helical scan performed with a given longitudinal collimation width and pitch.[20] Additional modifications were implemented to sample from all possible photon trajectories, taking into account scanner-specific fan angles and actual beam widths (as opposed to nominal collimation settings).[26] The energy of each simulated photon is obtained by sampling the energy spectrum of the scanner being simulated. Attenuation due to filtration (including the bowtie filter) is modeled by first using the filtration description for the particular scanner and bowtie filter setting being simulated to determine the distance the photon travels through the filter based on the photon's trajectory. Then, the resulting attenuation factor is calculated by assuming exponential attenuation and using the photon mass attenuation coefficient (μ/ρ) of the filtration material, also published by Hubbell and Seltzer,[29] and applied as an MCNPX source weight factor.

The scanner-specific energy spectra and filtration descriptions used for this work were generated using the "equivalent source" method described by Turner, *et al.*[26] The equivalent source model for a given scanner, bowtie filter, and kVp, consists of an equivalent energy spectrum and an equivalent bowtie filter description. The equivalent energy spectrum is numerically obtained so that its calculated half value layer (HVL) matches the measured HVL of the scanner, bowtie filter, and kVp combination of interest. The equivalent bowtie filter is one which attenuates the equivalent spectrum in a similar fashion as the actual filtration attenuates the actual x-ray beam, as determined by bowtie profile measurements (exposure values across the fan beam). As previously reported, $CTDI_{100}$ simulations performed using the equivalent source models generated for the scanner, bowtie filter, tube voltage (120 kVp), and collimation combinations used in this study agree with analogous physical measurements to within 1.6%, 1.4%, 1.0%, and 3.1% across center and periphery measurement positions for both the 16 and 32 cm diameter CTDI phantoms for scanners 1–4, respectively.

II.D. Organ dose simulations

II.D.1. Patient Model

For this work a single patient model was used for organ dose simulations based on "Irene," a member of the GSF family of voxelized phantoms.[14,25] The Irene data set consists of a three-dimensional matrix (262 columns × 132 rows × 348 slices) of organ identification numbers (e.g., organ codes) with voxel dimensions of $1.875 \times 1.875 \times 5.0$ mm^3 segmented from CT data of a patient with a height of 163 cm and a weight of 51 kg.[25] Each voxel was assigned a specific elemental composition and density within MCNPX based on its GSF organ code.

Twenty distinct materials, including various anatomical tissues defined by the ICRU Report 44 composition of body tissue tables,[30] air, and graphite (for the patient bed) were used in this work. For each material, the mass energy-absorption coefficients, $(\mu_{en}/\rho)_{material}$, necessary for the dose calculation described in Sec. II C 1 were generated for energies ranging from 1 to 120 keV. The $(\mu_{en}/\rho)_{material}$ values were each calculated as weighted averages of the elemental mass energy-absorption coefficients, $(\mu_{en}/\rho)_{element}$, for each element comprising the material, using the $(\mu_{en}/\rho)_{element}$ values published by Hubbell and Seltzer[29] and weights defined as the material's elemental percent composition given by either the ICRU report 44 tables[30] (for anatomical tissue) or by Hubbell and Seltzer[29] (for air).

II.D.2. Skeletal tissue doses

Red bone marrow (RBM) and bone surface (endosteal tissue) were not explicitly segmented in the Irene model, but homogeneous bone voxels were identified. The homogeneous bone (HB) composition and density (1.4 g/cm^3) of the adult ORNL phantoms (Oak Ridge, TN, Oak Ridge National Laboratory)[31] were used to describe all voxels designated as bone or skeleton. The dose to bone surface was approximated as the dose to the homogenous bone (D_{HB}), which was calculated under the assumption of CPE on a per photon basis as the product of the energy fluence ψ_{HB} in the skeleton voxel and the (μ_{en}/ρ) value for HB (obtained using the weighted average method described in Sec. II D 1 with the ORNL elemental composition serving as the weights). A method similar to that proposed by Rosenstein[32] was used to calculate dose to RBM. This approach estimates the deposited energy in RBM (E_{RBM}) by assuming

$$E_{RBM} = E_{HB} \times \frac{m_{RBM}}{m_{HB}} \times \frac{(\mu_{en}/\rho)_{RBM}}{(\mu_{en}/\rho)_{HB}}, \quad (2)$$

where E_{HB} is the energy deposited in HB, and m_{RBM} and m_{HB} are the total masses of RBM and HB in the phantom. By dividing both sides by m_{RBM} and noting that dose is the deposited energy divided by mass it can be seen that

$$D_{RBM} = D_{HB} \times \frac{(\mu_{en}/\rho)_{RBM}}{(\mu_{en}/\rho)_{HB}}. \quad (3)$$

As previously discussed, D_{HB} is calculated as the product of energy fluence in the skeleton voxel (ψ_{HB}) and $(\mu_{en}/\rho)_{HB}$, so dose to RBM was calculated on a per photon basis by

$$D_{RBM} = \psi_{HB} \times (\mu_{en}/\rho)_{RBM}. \quad (4)$$

II.D.3. Organ dose simulation experiments

For scanners 1–4, Monte Carlo simulations were performed using the Irene patient model and the equivalent source scanner models described above to obtain absorbed doses to the ICRP Publication 103 radiosensitive organs[5] from helical scans that utilized the scanning protocol described in Sec. II. For this feasibility study, the entire patient model (from top of head to bottom of feet) was included in the scan range. The scan length was determined by multiplying the longitudinal length of the voxels (5 mm) by the total number of slices (348), resulting in a 174 cm scan. This created a condition where each organ is completely encompassed in the scan region (and hence fully irradiated).

Because the Irene model was constructed with arms at her side and because most scans are performed with the patient's arms moved out of the field of view, all voxels belonging to the arms were set to air, effectively removing the arms from the scan. This results in a patient model condition that is obviously artificial, (especially when tallying dose to bone, bone marrow, skin, and muscle) but does allow the thorax, abdomen, and pelvic regions to undergo simulated scans without having the beam attenuated by arm tissue before reaching organs in the scan region.[33]

For each simulation, 10^9 photon histories were performed to ensure statistical simulation errors less than 1% for all organs. Dose was separately tallied in the 14 major and 11 remainder organs; it should be noted that the lymphatic nodes and oral mucosa (which are remainder organs) were not segmented in this GSF model.

As described in DeMarco *et al.*,[20] an exposure normalization factor is necessary to both convert MCNPX tally values from mGy/source particle to an absolute dose and to take into account the dependence of beam collimation on photon fluence. Exposure normalization factors were obtained for each scanner in units of source particle/total mA s, where total mA s is used to distinguish from mA s/rotation (mA s/rotation is typically the value entered at the scanner console and will be denoted as mA s). These factors were calculated as the ratio of 120 kVp $CTDI_{100}$ in-air measurements (mGy/total mA s) and corresponding 120 kVp $CTDI_{100}$ in-air simulations (mGy/source particle). The organ dose tally results were multiplied by the appropriate exposure normalization factor to obtain organ dose per total mA s (mGy/total mA s), where total mA s = mA s × number of rotations = mA s × (scan length/nominal collimation width). Finally, organ dose per mA s (mGy/mA s) were obtained by multiplying each organ dose per total mA s by the scan length divided by the scanner-specific nominal collimation width. In addition, the effective dose was calculated in mSv/mA s using the ICRP Publication 103 definition[5] in order to explore the variation in effective dose for a single patient model across scanners and investigate their normalization with measured $CTDI_{vol}$ values.

II.E. Analysis of organ dose values

II.E.1. Absorbed organ and effective doses

The Monte Carlo simulations resulted in unique absorbed dose values (in mGy/mA s) for each scanner and organ combination as well as effective doses (in mSv/mA s) for each scanner. These scanner-specific organ and effective dose values will be referred to as $D_{S,O}$ and $D_{S,\mathrm{ED}}$. For each organ, the mean absorbed dose across the four scanners, $\bar{D}_O$ (where $\bar{D}_O=\frac{1}{4}\Sigma_{S=1}^{4}D_{S,O}$), was calculated along with the standard deviation. Similarly, the mean effective dose across scanners, $\bar{D}_{\mathrm{ED}}$ (where $\bar{D}_{\mathrm{ED}}=\frac{1}{4}\Sigma_{S=1}^{4}D_{S,\mathrm{ED}}$) and the standard deviation were also computed. Finally, the coefficient of variation (CoV=standard deviation/mean) of the $D_{S,O}$ values for each organ as well as the $D_{S,\mathrm{ED}}$ values across scanners were calculated and expressed as a percentage.

II.E.2. Exploring the relationship between CTDI and organ (and effective) doses

Because $\mathrm{CTDI}_{\mathrm{vol}}$ and organ dose values appeared to vary in a similar fashion across scanners, the feasibility of reducing interscanner variability by normalizing organ doses by $\mathrm{CTDI}_{\mathrm{vol}}$ was explored. If successful, this would suggest the feasibility of an approach to estimating organ dose values across different scanners for a given patient based primarily on $\mathrm{CTDI}_{\mathrm{vol}}$ values.

To do this, each of the simulated organ dose values $D_{S,O}$ were normalized by the measured $\mathrm{CTDI}_{\mathrm{vol},S}$ value of the scanner being simulated. This resulted in a unitless quantity for each scanner and organ combination, referred to as $nD_{S,O}$ (where $nD_{S,O}=D_{S,O}/\mathrm{CTDI}_{\mathrm{vol},S}$). Then, for each organ, the mean $nD_{S,O}$ was calculated across scanners and denoted as $\overline{nD_O}$ (where $\overline{nD}_O=\frac{1}{4}\Sigma_{S=1}^{4}nD_{S,O}$). Similarly, the normalized effective dose values for each scanner $nD_{S,\mathrm{ED}}$ (where $nD_{S,\mathrm{ED}}=D_{S,\mathrm{ED}}/\mathrm{CTDI}_{\mathrm{vol},S}$, and the mean $nD_{S,\mathrm{ED}}$ across scanners, $\overline{nD}_{\mathrm{ED}}$ (where $\overline{nD}_{\mathrm{ED}}=\frac{1}{4}\Sigma_{S=1}^{4}nD_{S,\mathrm{ED}}$) were obtained. Finally, the coefficients of variation (CoVs) of the $nD_{S,O}$ values for each organ as well as the $nD_{S,\mathrm{ED}}$ values across scanners were calculated and expressed as a percentage.

III. RESULTS

The CTDI measurements obtained with the 32 cm (body) CTDI phantom using a tube voltage of 120 kVp and the widest possible scanner collimation for each scanner are reported in Table I on a per mA s basis. For scanners 1–4 the scanner-specific center and periphery $\mathrm{CTDI}_{100,S}$ measurements are shown in the first two columns and the $\mathrm{CTDI}_{\mathrm{vol},S}$ values for pitch 1 are displayed in the last column. This table shows that there is considerable variation between scanners in terms of $\mathrm{CTDI}_{\mathrm{vol},S}$; scanner 4 has a $\mathrm{CTDI}_{\mathrm{vol},S}$ value that is nearly twice that of scanners 1 and 2 and scanner 3 is nearly 50% higher than scanners 1 and 2. This table also shows the mean, standard deviation and coefficient of variation (CoV expressed as a percentage) for each CTDI value across scanners. Specifically for $\mathrm{CTDI}_{\mathrm{vol},S}$, the mean, standard deviation, and CoV are 0.084 mGy/mA s, 0.029 mGy/mA s, and 34.1%, respectively.

TABLE I. CTDI measurements for scanners 1–4. All values in mGy/mA s.

	$\mathrm{CTDI}_{100,S}$		
Scanner	Center	Periphery	$\mathrm{CTDI}_{\mathrm{vol},S}$
1	0.040	0.074	0.063
2	0.037	0.075	0.062
3	0.051	0.107	0.089
4	0.069	0.150	0.123
Mean	0.049	0.102	0.084
Standard deviation	0.014	0.036	0.029
CoV (%)	28.8%	35.4%	34.1%

The organ doses $D_{S,O}$ (in mGy/mA s) and effective doses $D_{S,\mathrm{ED}}$ (in mSv/mA s) described in Sec. II E 1 for scanners 1–4 are plotted in Fig. 1 and displayed in Table II (the table explicitly lists doses for all ICRP Publication 103 radiosensitive organs, while the plot displays doses for the 14 major organs and the average dose of the 11 remainder organs). It can be seen from Fig. 1 that, for most organs, there is a considerable difference in dose values between some of the different scanners. For example, the dose to most organs from scanner 4 is approximately twice that of scanner 2. With the exception of scanners 1 and 2, this relatively large variation appears fairly consistent for other pairwise scanner comparisons across most organs. Table II quantifies this variation by reporting the mean organ doses ($\bar{D}_O$ and $\bar{D}_{\mathrm{ED}}$), the standard deviation, and the CoV across scanners. The minimum variation was approximately 26.7% (for the adrenals) and the maximum was approximately 37.7% (for the thyroid), with a mean CoV of about 31.6%. In addition, the table shows that the mean effective dose across scanners is 0.15 mSv/mA s with a CoV of 31.5%.

The $\mathrm{CTDI}_{\mathrm{vol}}$ normalized organ ($nD_{S,O}$) and effective doses ($nD_{S,\mathrm{ED}}$) for scanners 1–4 ($D_{S,O}$ and $D_{S,\mathrm{ED}}$ normalized by $\mathrm{CTDI}_{\mathrm{vol},S}$ as described in Sec. II E 2) are plotted in Fig. 2 and displayed in Table III (the table explicitly lists $nD_{S,O}$ values for all ICRP Publication 103 radiosensitive organs, while the plot displays $nD_{S,O}$ values for the 14 major organs and the average value of the 11 remainder organs). Unlike the results in previous sections, Table III and Fig. 2 show very little difference in $\mathrm{CTDI}_{\mathrm{vol}}$ normalized dose values between different scanners. For example, the $\mathrm{CTDI}_{\mathrm{vol}}$ normalized dose to most organs from scanner 4 is within 10%–15% of those of all other scanners. Table III quantifies this reduced variation by reporting the mean $\mathrm{CTDI}_{\mathrm{vol}}$ normalized organ ($\overline{nD_O}$) or effective doses ($\overline{nD}_{\mathrm{ED}}$), the standard deviation, and the coefficient of variation across scanners. The bottom three rows of Table III display the mean, maximum, and minimum coefficient of variation across all organs of the $\mathrm{CTDI}_{\mathrm{vol}}$ normalized dose values. The mean variation was approximately 5.2%, with a minimum of approximately 2.4% (for skin tissue) and a maximum of approximately 8.5% (for the adrenals).

A quantitative comparison of the last column of Table III with that of Table II indicates that for all organs the variations in the $\mathrm{CTDI}_{\mathrm{vol}}$ normalized dose values across scanners

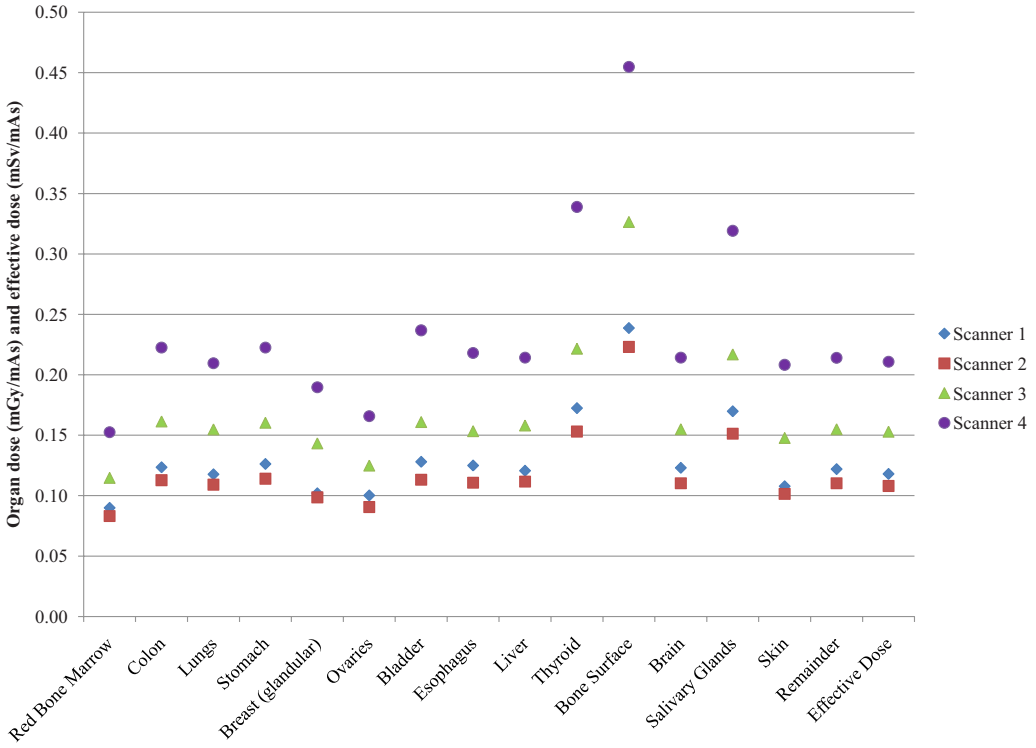

FIG. 1. Organ dose ($D_{S,O}$) in mGy and effective dose ($D_{S,ED}$), in mSv, for a 100 mA s/rot scan for scanners 1–4.

are much smaller than those of the un-normalized doses. Specifically, it can be seen that for all organs the CoV values across scanners of the $CTDI_{vol}$ normalized doses are less than those of the un-normalized values. Comparison of the summary statistics in the bottom three rows of Tables II and III further illustrates that organ doses normalized by $CTDI_{vol}$ have a smaller variation across scanners than do un-normalized dose values. Furthermore, the relatively small variance of the $CTDI_{vol}$ normalized doses (the maximum CoV was 8.5%) indicates that, for any organ, the mean value ($\overline{nD_O}$) is a good approximation of the value for any individual 64-slice MDCT scanner ($nD_{S,O}$). Therefore, since the product of the generic $\overline{nD_O}$ and a particular scanner's measured $CTDI_{vol}$ will result in a scanner-specific dose, these findings demonstrate the feasibility of a *scanner-independent* technique to estimate organ dose based on standard $CTDI_{vol}$ to dose conversion coefficients.

IV. DISCUSSION

The purpose of this study was to investigate the feasibility of a method to estimate organ doses that is scanner-independent by assessing the ability of $CTDI_{vol}$ measurements to account for differences in MDCT scanners that lead to organ dose differences. In the first set of results, Table I showed large variations in $CTDI_{vol}$ between scanners, with a CoV of 34.1%. In the simulation experiments, the analysis of the un-normalized organ and effective doses ($D_{S,O}$ and $D_{S,ED}$) from scanners 1–4 demonstrated differences across scanners that were very similar to those observed in the $CTDI_{vol}$ values. The results in Table II and the plot in Fig. 1 definitively illustrate this variation. Scanner 4 delivered the highest doses, by a relatively large margin, for all the radiosensitive organs used in this study. Scanner 3's dose values were typically 65%–75% of scanner 4's while scanners 1 and 2, which actually resulted in similar doses, were on the order of 45%–60% of scanner 4's doses. Overall, the CoV across scanners for a given organ ranged between 26.7% (for the adrenals) to 37.7% (for the thyroid), with a mean 31.6% across all organs.

It should be emphasized that both $CTDI_{vol}$ and absolute organ doses were reported on a per mA s basis. As a result, dose differences can attributed to differences in filtration designs including bowtie filter thickness, composition, and shape (which results in differences in x-ray output characteristics).[26] Furthermore, calculating organ doses on a per mA s basis did not allow organ dose comparisons to be made for exams with equivalent image quality. The actual mA s values necessary to achieve comparable image quality will almost certainly vary depending on the scanner. Instead, this work was carried out in order to consider the feasibility of normalizing out organ dose differences on a *per* mA s basis between scanners via $CTDI_{vol}$ measurements.

Because both $CTDI_{vol}$ and organ doses exhibited similar cross-scanner variations, the normalization of the organ and effective doses by $CTDI_{vol,S}$ measurements were investigated. The resulting normalized values, $nD_{S,O}$ and $nD_{S,ED}$, were presented in Fig. 2 and Table III. The $nD_{S,O}$ and $nD_{S,ED}$ values had much less variation across scanners relative to the un-normalized dose values. This point is emphasized by the noticeable convergence of points in Fig. 2 compared to the spread of the points in Fig. 1, and is indeed consistent with the observations of Shrimpton in his comparisons of effec-

TABLE II. Organ dose ($D_{S,O}$) in mGy/mA s and effective dose ($D_{S,ED}$), in mSv/mA s for scanners 1–4. Columns 6–8 display the mean, standard deviation, and CoV across scanners. The bottom three rows display the mean, maximum, and minimum of the CoV across organs.

Organ	Scanners 1	2	3	4	Mean ($\bar{D}_{S,O}$)	Standard deviation	CoV (%)
Red bone marrow	0.09	0.08	0.11	0.15	0.11	0.03	28.5
Colon	0.12	0.11	0.16	0.22	0.16	0.05	32.0
Lungs	0.12	0.11	0.15	0.21	0.15	0.05	31.0
Stomach	0.13	0.11	0.16	0.22	0.16	0.05	31.2
Breast (glandular)	0.10	0.10	0.14	0.19	0.13	0.04	32.0
Ovaries	0.09	0.09	0.12	0.17	0.12	0.04	31.6
Bladder	0.13	0.11	0.16	0.24	0.16	0.06	34.5
Esophagus	0.12	0.11	0.15	0.22	0.15	0.05	31.4
Liver	0.12	0.11	0.16	0.21	0.15	0.05	30.8
Thyroid	0.17	0.15	0.22	0.34	0.22	0.08	37.7
Bone surface	0.24	0.22	0.33	0.45	0.31	0.11	34.2
Brain	0.12	0.11	0.15	0.21	0.15	0.05	30.8
Salivary glands	0.17	0.15	0.22	0.32	0.21	0.08	35.1
Skin	0.11	0.10	0.15	0.21	0.14	0.05	34.8
Adrenals	0.11	0.10	0.14	0.19	0.14	0.04	26.7
Extrathoracic region	0.13	0.12	0.17	0.24	0.16	0.05	31.8
Gall bladder	0.13	0.12	0.17	0.24	0.16	0.05	31.8
Heart	0.14	0.12	0.17	0.24	0.17	0.05	32.2
Kidney	0.11	0.11	0.15	0.20	0.14	0.04	29.2
Muscle	0.11	0.10	0.15	0.20	0.14	0.04	31.8
Pancreas	0.11	0.10	0.14	0.19	0.13	0.04	28.6
Small intestine	0.12	0.11	0.15	0.22	0.15	0.05	32.1
Spleen	0.12	0.11	0.15	0.21	0.15	0.04	30.5
Thymus	0.14	0.12	0.18	0.26	0.17	0.06	34.3
Uterus	0.11	0.10	0.14	0.19	0.14	0.04	30.2
Effective dose	0.12	0.11	0.15	0.21	0.15	0.05	31.5
						Mean CoV:	**31.6**
						Max. CoV:	**37.7**
						Min. CoV:	**26.7**

tive dose normalized by $CTDI_w$ using older scanners.[16] The CoV across scanners for a given organ ranged from 2.4% (for skin tissue) to 8.5% (for the adrenals), with a mean across all organs of 5.2%. This is a drastic reduction compared to the mean CoV of 31.6% seen for the un-normalized doses. These results indicate that the characteristics of a scanner that influence organ dose, such as filtration designs, influence $CTDI_{vol}$ values in a similar fashion and that normalizing by $CTDI_{vol}$ effectively accounts for these differences across scanners. Specifically, for any organ, the $CTDI_{vol}$ normalized dose for a particular 64-slice MDCT scanner will be within approximately 10% of the mean value across all 64-slice MDCT scanners (i.e., $nD_{S,O}=\overline{nD}_O+10\%$).

The relatively small variance of the organ dose normalized by $CTDI_{vol}$ values suggests that, for a given patient, anatomical scan region, and scan protocol (i.e., tube voltage and bowtie size), it is feasible to estimate organ doses from any 64-slice scanner based on a single set of scanner-independent $CTDI_{vol}$ to dose conversion coefficients. Quantitatively, the CoV of 5.2% indicates that multiplying the $\overline{nD}_{S,O}$ or $\overline{nD}_{S,ED}$ values by the scanner-specific $CTDI_{vol}$ value (in mGy/mA s) and the relevant mA s used clinically, it is possible, on average, to estimate absolute organ or effective doses to within approximately 10% accuracy for any 64-slice MDCT scanner.

This study was meant to demonstrate that scanner-specific dependencies are accounted for when $CTDI_{vol}$ measurements are used as normalization factors for organ doses. The results suggest the *feasibility* that scanner-independent organ dose conversion coefficients can be generated for patient-specific and protocol-specific scans. In this work organs were fully irradiated with no extra attenuation from arm tissue in order to mimic the primary x-ray fluence conditions of a typical CT exam (i.e., moving the arms up for a chest or abdomen scan). Head to toe scans were performed to ensure the conclusions of this work applied to all radiosensitive organs in the body. The results show that for all organs, the $nD_{S,O}$ values have little variation across scanners; however, it should be emphasized that the $\overline{nD}_O$ values reported in this study are not intended to serve as actual $CTDI_{vol}$ to organ dose coefficients. The fact that the arms were removed indicates that the results are not applicable for a true full-body exam where the $\overline{nD}_O$ values would be larger for tissues found in the arms, such as skin, muscle, RBM, and bone surface,

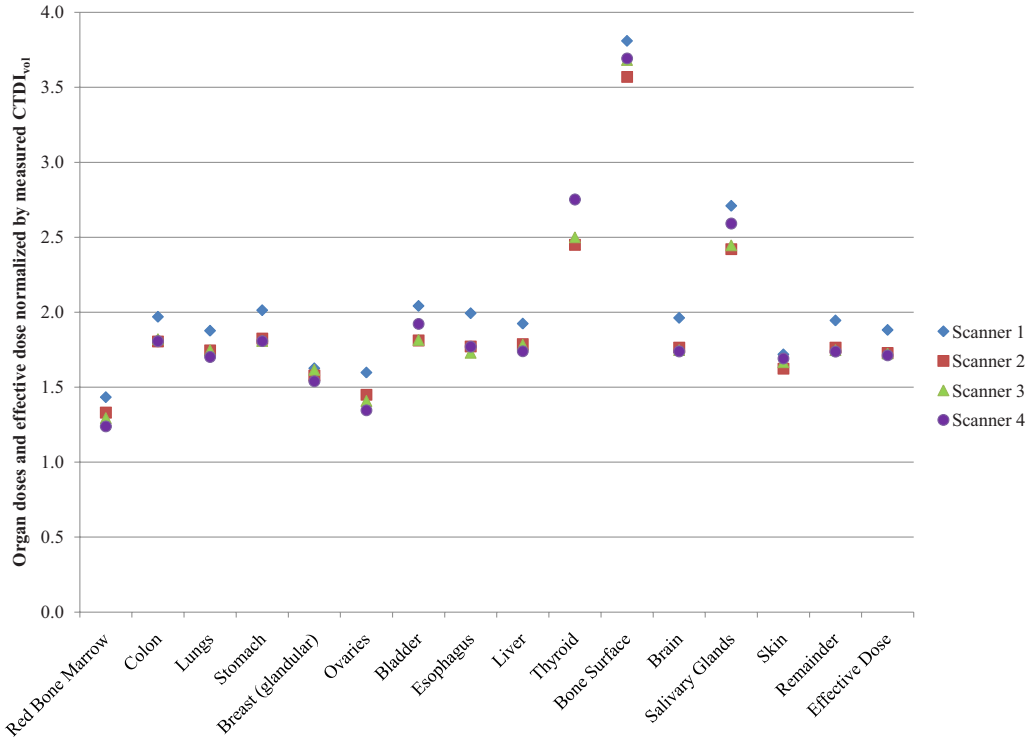

FIG. 2. $CTDI_{vol}$, S normalized organ ($nD_{S,O}$), and effective ($nD_{S,ED}$) doses for scanners 1–4.

and smaller for organs that would receive less radiation due to arm attenuation. Furthermore, the reported $\overline{nD}_O$ values may not be appropriate even for fully irradiated organs in partial-body exams (i.e., stomach in an abdomen scan) as scatter from distant anatomy that would not be irradiated for a partial-body scan is included in these simulations. Finally, the results of this work are limited to the particular patient model and scan protocol (tube voltage, bowtie filter, collimation, and pitch) used in the simulations. These limitations will all be addressed in future studies to extend the $CTDI_{vol}$ to organ dose estimation method proposed here.

Another limitation is that the patient model used in this study, Irene of the GSF family of models, did not include separately segmented RBM and bone surface (endosteal layer) anatomy, so the dose to these skeletal tissues could not be directly simulated. The two-term mass energy-absorption coefficient method used to approximate skeletal doses, described in Sec. II D 2, was evaluated by Lee *et al.*[34] and found to overestimate RBM dose at the energies used in this study. Therefore, $CTDI_{vol}$ to dose conversion coefficients for skeletal tissue will be investigated in future studies using voxelized phantoms with explicitly segmented cortical bone and spongiosa regions[35] along with bone-specific and bone-region-specific photon fluence-to-dose response functions.[36]

Future Monte Carlo studies will be conducted using multiple computational anthropomorphic phantoms representing a range of different patients in order to examine the effect of size, body habitus, and gender on $CTDI_{vol}$ to dose conversion coefficients and develop methods to account for these effects. Partial-body scans will be performed using several different sized patient models. This will help identify potential complications for generating $CTDI_{vol}$ to dose conversion coefficients, including the effects on organs not fully encompassed in the scan region (i.e., those that are partially irradiated such as the lower intestine in an abdominal scan). Additionally, methods to take into account variations in the scanning protocol, such as different pitch, bowtie filter sizes, and collimation settings, will be investigated. Finally, since the majority of current clinical exams use tube current modulation (TCM) schemes in order to reduce dose levels, the effect of TCM will be explored in a manner similar to that reported by Angel, *et al.*[38,39] in order to devise an approach to account for the resulting organ dose reduction. If these issues can be resolved, it should be feasible to produce a truly universal set of patient-independent and scanner-independent $CTDI_{vol}$ to organ dose conversion coefficients for a range of scan protocols that can be implemented to quickly and accurately estimate patient dose from any CT exam. In addition, there have been discussions concerning the revision of standardized CT dosimetry measurements, especially for exams performed with wider beams (40–180 mm).[37] When developed, these revised index values will be investigated as organ dose normalization factors for scanners and exams that CTDI may not adequately characterize.

While the focus of this manuscript is on assessing radiation dose from CT, it should be pointed out that CT scans are a very important tool for diagnosis and assessment of response to treatment in the practice of medicine. Technical developments have led to an expanding list of applications that have supplanted less accurate or more invasive diagnostic tests[40] (such as exploratory surgery), which in turn has led to a dramatic increase in the use of body CT.[1] The detailed

TABLE III. $CTDI_{vol}$ normalized organ ($nD_{S,O}$) and effective ($nD_{S,ED}$) dose values for scanners 1–4. Columns 6–8 display the mean, standard deviation, and CoV across scanners. The bottom three rows display the mean, maximum, and minimum of the CoV across organs.

Organ	Scanners 1	2	3	4	Mean ($\overline{nD_{S,O}}$)	Standard deviation	CoV (%)
Red bone marrow	1.43	1.33	1.29	1.24	1.32	0.08	6.2
Colon	1.97	1.80	1.82	1.81	1.85	0.08	4.3
Lungs	1.88	1.75	1.75	1.70	1.77	0.08	4.3
Stomach	2.01	1.82	1.81	1.81	1.86	0.10	5.4
Breast (glandular)	1.63	1.58	1.62	1.54	1.59	0.04	2.5
Ovaries	1.48	1.40	1.41	1.37	1.42	0.05	7.4
Bladder	2.04	1.81	1.82	1.92	1.90	0.11	5.7
Esophagus	1.99	1.77	1.73	1.77	1.82	0.12	6.6
Liver	1.92	1.79	1.78	1.74	1.81	0.08	4.4
Thyroid	2.75	2.45	2.50	2.75	2.61	0.16	6.2
Bone surface	3.81	3.57	3.68	3.69	3.69	0.10	2.7
Brain	1.96	1.76	1.75	1.74	1.80	0.11	5.9
Salivary glands	2.71	2.42	2.45	2.59	2.54	0.13	5.3
Skin	1.72	1.62	1.67	1.69	1.68	0.04	2.4
Adrenals	1.83	1.65	1.59	1.50	1.64	0.14	8.5
Extrathoracic region	2.09	1.92	1.93	1.91	1.96	0.09	4.3
Gall bladder	2.13	1.91	1.89	1.92	1.96	0.11	5.8
Heart	2.20	1.96	1.94	1.99	2.02	0.12	5.9
Kidney	1.83	1.70	1.68	1.61	1.71	0.09	5.5
Muscle	1.74	1.63	1.64	1.61	1.65	0.06	3.4
Pancreas	1.78	1.59	1.54	1.51	1.60	0.12	7.8
Small intestine	1.93	1.73	1.74	1.75	1.79	0.09	5.3
Spleen	1.84	1.73	1.73	1.67	1.74	0.07	4.1
Thymus	2.25	1.97	2.00	2.10	2.08	0.13	6.0
Uterus	1.78	1.60	1.55	1.56	1.62	0.11	6.7
Effective dose	1.88	1.73	1.73	1.71	1.76	0.08	4.6
						Mean CoV:	**5.2**
						Max. CoV:	**8.5**
						Min. CoV:	**2.4**

assessment of anatomy and function that CT imaging provides does require the use of x rays, which do result in some small, but not zero, risk to patients. In the vast majority of cases, the benefits do significantly outweigh the risks in having a CT exam performed.

The pertinent conclusions from this work are that: (a) There is considerable variation among modern MDCT scanners when considering both organ and effective dose (on the order of ~200% in some cases) and (b) this variation can be mostly accounted for by using scanner-specific $CTDI_{vol}$ measurements as a normalization factor. The first of these conclusions implies the difficulty of applying absolute dose values from Monte Carlo studies performed for a particular scanner model to other scanners. However, the second conclusion suggests that by normalizing organ doses by measured $CTDI_{vol}$ values, the characteristics that differentiate the simulated scanner from other scanners can be accounted for, producing a normalized organ dose that can be applied to a range of MDCT scanners. Future MDCT organ dose studies should utilize this finding by reporting organ and effective doses on a per measured $CTDI_{vol}$ basis. This work represents the first step in establishing a universal organ dose framework for MDCT scanners which utilizes $CTDI_{vol}$ to account for the scanner-specific dependencies of organ and effective dose. The future studies discussed above will expand this framework to include the effects of patient size, pitch, and scan region considerations with the ultimate goal of estimating organ dose to any patient from any scanner through the use of universal $CTDI_{vol}$ to dose conversion coefficients.

[a]Electronic mail: aturner@mednet.ucla.edu

[1]F. A. Mettler, Jr., B. R. Thomadsen, M. Bhargavan, D. B. Gilley, J. E. Gray, J. A. Lipoti, J. McCrohan, T. T. Yoshizumi, and M. Mahesh, "Medical radiation exposure in the U.S. in 2006: Preliminary results," Health Phys. **95**(5), 502–507 (2008).

[2]National Research Council, *Health Risks from Exposure to Low Levels of Ionizing Radiation: BEIR VII Phase 2* (The National Academies Press, Washington, DC, 2005).

[3]American Association of Physicists in Medicine, "The measurement, reporting and management of radiation dose in CT," AAPM Report No. 96 (New York, 2008).

[4]International Commission on Radiological Protection and Measurements, "1990 Recommendations of the International Commission on Radiological Protection," *ICRP Publication 60* (International Commission on Radiological Protection, Essen, 1990).

[5]International Commission on Radiological Protection, "The 2007 Recommendations of the International Commission on Radiological Protection,"

ICRP Publication 103 (International Commission on Radiological Protection, Essen, 2007).
[6]E. J. Hall and D. J. Brenner, "Cancer risks from diagnostic radiology," Br. J. Radiol. **81**(965), 362–378 (2008).
[7]C. H. McCollough, "CT dose: How to measure, how to reduce," Health Phys. **95**(5), 508–517 (2008).
[8]M. F. McNitt-Gray, "AAPM/RSNA physics tutorial for residents: Topics in CT—Radiation dose in CT," Radiographics **22**(6), 1541–1553 (2002).
[9]D. J. Brenner and C. H. McCollough, "It is time to retire the computed tomography dose index (CTDI) for CT quality assurance and dose optimization?," Med. Phys. **33**(5), 1189–1191 (2006).
[10]D. G. Jones and P. C. Shrimpton, "Survey of CT practice in UK. Part 3: Normalized organ doses calculated using Monte Carlo techniques," National Radiological Protection Board Report No. R250, 1991 (unpublished).
[11]M. Zankl, W. Panzer, and G. Drexler, "The calculation of dose from external photon exposures using reference human phantoms and Monte Carlo methods. VI. Organ doses from computed tomographic examinations," GSF Report No. 30/91 (GSF-Forschungszentrum, Oberschleissheim, Germany, 1991).
[12]Imaging Performance Assessment of CT Scanners Group, "ImPACT CT patient dosimetry calculator," 2006, available at http://www.impactscan.org.
[13]G. Stamm and H. D. Nagel, "CT-Expo—A novel program for dose evaluation in CT [in German]," Rofo Fortschr Geb Rontgenstr Neuen Bildgeb Verfahr **174**, 1570–1576 (2002).
[14]N. Petoussi-Henss, M. Zankl, U. Fill, and D. Regulla, "The GSF family of voxel phantoms," Phys. Med. Biol. **47**, 89–106 (2002).
[15]M. Salvado, M. Lopez, J. J. Morant, and A. Calzado, "Monte Carlo calculation of radiation dose in CT examinations using phantom and patient tomographic models," Radiat. Prot. Dosim. **114**(1–3), 364–368 (2005).
[16]P. C. Shrimpton, "Assessment of patient dose in CT," NRPB Report No. PE/1/2004 (National Radiological Protection Board, Chilton, UK, 2004).
[17]K. A. Jessen, P. C. Shrimpton, J. Geleijns, W. Panzer, and G. Tois, "Dosimetry for optimisation of patient protection in computed tomography," Appl. Radiat. Isot. **50**, 165–172 (1999).
[18]K. A. Jessen *et al.*, *EUR 16262: European Guidelines on Quality Criteria for Computed Tomography* (Office for Official Publications of the European Communities, Luxembourg, 2000).
[19]P. C. Shrimpton, M. C. Miller, M. A. Lewis, and M. Dunn, "Doses from computed tomography (CT) examinations in the UK–2003 review," NRPB Report No. W67 (National Radiological Protection Board, Chilton, UK, 2005).
[20]J. J. DeMarco, C. H. Cagnon, D. D. Cody, D. M. Stevens, C. H. McCollough, J. O'Daniel, and M. F. McNitt-Gray, "A Monte Carlo based method to estimate radiation dose from multidetector CT (MDCT): Cylindrical and anthropomorphic phantoms," Phys. Med. Biol. **50**, 3989–4004 (2005).
[21]B. Schmidt and W. A. Kalendar, "A fast voxel-based Monte Carlo method for scanner- and patient-specific doe calculations in computed tomography," Phys. Med. **18**, 43–53 (2002).
[22]A. Tzedakis, J. Damilakis, K. Perisinakis, J. Stratakis, and N. Gourtsoyiannis, "The effect of z overscanning on patient effective dose calculated for CT examinations," Med. Phys. **32**(6), 1621–1629 (2005).
[23]R. J. Staton, C. Lee, C. Lee, M. D. Williams, D. E. Hintenlang, M. M. Arreola, J. L. Williams, and W. E. Bolch, "Organ and effective doses in newborn patients during helical multislice computed tomography examination," Phys. Med. Biol. **51**, 5151–5166 (2006).
[24]J. Gu, B. Bednarz, P. F. Caracappa, and X. G. Xu, "The development, validation and application of a multi-detector CT (MDCT) scanner model for assessing organ doses to the pregnant patient and the fetus using Monte Carlo simulations," Phys. Med. Biol. **54**, 2699–2717 (2009).
[25]U. A. Fill, M. Zankl, N. Petoussi-Henss, M. Siebert, and D. Regulla, "Adult female voxel models of different stature and photon conversion coefficients for radiation protection," Health Phys. **86**(3), 253–272 (2004).
[26]A. Turner, D. Zhang, H. J. Kim, J. J. DeMarco, C. H. Cagnon, E. Angel, D. D. Cody, D. M. Stevens, A. N. Primak, C. H. McCollough, and M. F. McNitt-Gray, "A method to generate equivalent energy spectra and filtration models based on measurement for multidetector CT Monte Carlo dosimetry simulations," Med. Phys. **36**(6), 2154–2164 (2009).
[27]L. Waters, "MCNPX User's Manual, Version 2.4.0," Los Alamos National Laboratory Report No. LA-CP-02-408, 2002.
[28]L. Waters, "MCNPX Version 2.5.C," Los Alamos National Laboratory Report No. LA-UR-03-2202 (2003).
[29]J. H. Hubbell and S. M. Seltzer, "Tables of x-ray mass attenuation coefficients and mass energy-absorption coefficients," (online) (National Institute of Standards and Technology, Gaithersburg, MD, 1996), available at http://physics.nist.gov/PhysRefData/XrayMassCoef/cover.html.
[30]ICRU, "Tissue substitutes in radiation dosimetry and measurement," The International Commission on Radiation Units and Measurements, Report No. 44 (ICRU, Bethesda, MD, 1989).
[31]M. Cristy and K. F. Eckerman, "Specific absorbed fractions of energy at various ages from internal photon sources," ORNL Report No. TM-8381 (Oak Ridge National Laboratory, Oak Ridge, TN, 1987), Vol. I–VII.
[32]M. Rosenstein, "Organ doses in diagnostic radiology," HEW Publication FDA 76–8030 (Food and Drug Administration, Rockville, MD, 1976).
[33]D. Zhang, A. S. Savandi, J. J. DeMarco, C. H. Cagnon, E. A. Angel, A. C. Turner, D. D. Cody, D. M. Stevens, A. N. Primak, C. H. McCollough, and M. F. McNitt-Gray, "Variability of surface and center position in MDCT: Monte Carlo simulations using CTDI and anthropomorphic phantoms," Med. Phys. **36**(3), 1025–1038 (2009).
[34]C. Lee, C. Lee, A. P. Shah, and W. E. Bolch, "An assessment of bone marrow and bone endosteum dosimetry methods for photon sources," Phys. Med. Biol. **51**, 5391–5407 (2006).
[35]M. Zankl, K. F. Eckerman, and W. E. Bolch, "Voxel-based models representing the male and female ICRP reference adult—The skeleton," Radiat. Prot. Dosim. **127**(1–4), 174–186 (2007).
[36]K. F. Eckerman, W. E. Bolch, M. Zankl, and N. Petoussi-Henss, "Response functions for computing absorbed dose to skeletal tissues from photon irradiation," Radiat. Prot. Dosim. **127**(1–4), 187–191 (2007).
[37]R. L. Dixon, "A new look at CT dose measurement: Beyond CTDI," Med. Phys. **30**, 1272–1280 (2003).
[38]E. Angel, N. Yaghmai, C. M. Jude, J. J. DeMarco, C. H. Cagnon, J. G. Goldin, C. H. McCollough, A. N. Primak, D. D. Cody, D. M. Stevens, and M. F. McNitt-Gray, "Dose to radiosensitive organs during routine chest CT: Effects of tube current modulation," AJR, Am. J. Roentgenol. **193**(5), 1340–1345 (2009).
[39]E. Angel, N. Yaghmai, C. M. Jude, J. J. DeMarco, C. H. Cagnon, J. G. Goldin, A. N. Primak, D. M. Stevens, D. D. Cody, C. H. McCollough, and M. F. McNitt-Gray, "Monte Carlo simulations to assess the effects of tube current modulation on breast dose for multidetector CT," Phys. Med. Biol. **54**(3), 497–512 (2009).
[40]C. H. McCollough, L. Guimarães, and J. G. Fletcher, "In defense of body CT," AJR, Am. J. Roentgenol. **193**(1), 28–39 (2009).